

A. Klein, H. Carfantan, D. Testa, A. Fasoli, J. Snipes and JET EFDA contributors

A New Method for the Analysis of Magnetic Fluctuations in Unevenly-Spaced Mirnov Coils

"This document is intended for publication in the open literature. It is made available on the understanding that it may not be further circulated and extracts or references may not be published prior to publication of the original when applicable, or without the consent of the Publications Officer, EFDA, Culham Science Centre, Abingdon, Oxon, OX14 3DB, UK."

"Enquiries about Copyright and reproduction should be addressed to the Publications Officer, EFDA, Culham Science Centre, Abingdon, Oxon, OX14 3DB, UK."

A New Method for the Analysis of Magnetic Fluctuations in Unevenly-Spaced Mirnov Coils

A. Klein¹, H. Carfantan², D. Testa³, A. Fasoli³, J. Snipes¹
and JET EFDA contributors*

JET-EFDA, Culham Science Centre, OX14 3DB, Abingdon, UK

¹*MIT Plasma Science and Fusion Center, Cambridge, MA 02139, USA*

²*Laboratoire Astrophysique de Toulouse Tarbes, CNRS/Université Paul Sabatier Toulouse 3, Toulouse, France*

³*CRPP, Association EURATOM – Confédération Suisse, EPFL, Lausanne, Switzerland*

** See annex of M.L. Watkins et al, "Overview of JET Results ",
(Proc. 21st IAEA Fusion Energy Conference, Chengdu, China (2006)).*

ABSTRACT

Analysis of magnetic fluctuations external to toroidal plasmas is important for understanding the magneto-hydrodynamic (MHD) properties of the plasma, among other things. These properties affect nearly all aspects of behavior of magnetic confinement, and thus are of interest in topics ranging from gross global plasma stability, control, and disruption avoidance, to the more subtle areas such as are involved with passive and active MHD spectroscopy, to name a few examples. Mode number analysis is generally accomplished by interpreting signals from a finite number of external Mirnov coils, which typically are unevenly spaced in the toroidal and poloidal coordinates. The toroidal mode number, n , is usually easily determined in tokamaks because different modes generally oscillate at well separated and distinct frequencies, because of toroidal symmetry, and because n is often very low ($n \leq 2$). On occasion however, multiple modes of various origins may overlap in frequency, and then the signals in the individual sensors are the result of a superposition of multiple modes, so that the task of spatial decomposition becomes a difficult problem. Previous efforts to resolve mode numbers involve phase fitting, singular value decomposition and/or Lomb periodogram techniques. We describe a new approach, based on the SparSpec method, and show that it may be superior in several respects. To illustrate the method, we apply SparSpec to data from externally driven, stable Alfvén Eigenmodes on the JET device.

1. BACKGROUND AND DESCRIPTION OF SPARSPEC

The variety of methods in common use to determine the spatial structure of MHD phenomena in toroidal plasmas from external magnetic measurements is quite small. In the standard tokamak coordinate system, magnetic perturbations at the plasma edge are represented well by functions involving toroidal and poloidal harmonics, written as $\psi_{m,n} = e^{i(n\phi)} \sum_m e^{i(m\theta)}$, where each mode has one single toroidal mode number, but will include several poloidal Fourier harmonics due to toroidicity and other geometric effects. As a result, the poloidal quantum number is not well defined, even in very large aspect ratio plasmas with cylindrical cross-section. In the poloidal dimension, uniform spacing between sensors does not result in any gain in terms of ease of analysis, because the distance between sensor and plasma surface is invariably a function of poloidal angle θ , and because a Shafranov shift and plasma shaping effects will result in effective spacing periods $\Delta\theta$ that are anything but constant. Additionally, because poloidal mode-structure can never be represented by a single Fourier term, a technique such as Singular Value Decomposition (SVD) is appropriate, since it makes no assumptions about the nature of the spatial basis functions [1].

For the toroidal aspect of the analysis however, the eigenfunctions describing perturbations are best represented by simple sinusoids. When sensors are evenly spaced in the toroidal dimension, a simple discrete Fourier transform will reveal the mode amplitudes for each n separately [2], up to the Nyquist mode number given by $n_{\max} = \pi/\Delta\phi$ (here $\Delta\phi$ is the angle between adjacent probes). Unfortunately, evenly spaced sensors are often not available due to engineering constraints. Furthermore, it can be shown that even spacing does not represent an optimum arrangement for

magnetic pickup coils, because of the aforementioned Nyquist limitations and aliasing effects [3]. Therefore, the standard approach for determining the n-number of an MHD mode is to fit the phases of data from two or more sensors separated by their toroidal angle to a straight line. The slope of the line then represents the n-number.

When there is only one dominant mode with one single n-number, phase-fitting is relatively successful and simple (i.e., fast), but when there are multiple modes with multiple n-numbers some other means to resolve the mode numbers must be used. The tools employed to estimate sinusoidal contributions in sets of unevenly sampled data have traditionally involved the so-called Lomb periodogram [4], and this method was recently applied to Alfvén Eigenmode identification in the Wendelstein 7-AS stellarator [5]. This is essentially a Least Squares (LS) fitting to sinusoids, which works well if there is only one dominant mode, but has limitations when multiple modes are present in the data. LS fitting of sinusoids from unevenly sampled series is a difficult problem because of the non-linearity of the model with respect to the mode number parameters, so the LS criterion may have many local minima in which optimization algorithms may get stuck (while the global minimum is required). For a single mode number, it leads to the maximization of the Lomb periodogram, but the problem is generally more difficult for several modes, even if the number of modes is known (which is rarely the case).

A recent publication by Hole and Appel [6] describes an approach which uses SVD methods to fit magnetic data to a predetermined number (M) of Fourier modes. This approach is capable in principle of finding multiple simultaneous modes (degenerate in frequency) by LS fitting to a set of sinusoidal basis functions after testing all linear combinations of these basis functions, computing the least square solution for each, and selecting the one with the smallest residual as defined in [6]. The drawbacks of this method are twofold: First, for M higher than 1, the number of detected modes will always be M , even if there is only one mode in the data. (However, the additional modes will have a low amplitude.) Second, for $M > 1$, it rapidly becomes computationally expensive to run through all possible combinations of M modes, the number of which is given by the binomial coefficient, $n! \div M!(n-M)!$ (here n is the maximum allowed mode number). For example, for the maximum n-number limited to $n \leq 20$, there are respectively 820, 10,660, 101,270 and 749,398 combinations, for $M = 2, 3, 4$ and 5 . For $n_{\max} = 30$ and $M = 5$, there are 5,949,147 combinations! Although the computation of the Moore-Penrose pseudo-inverse matrices can be done just once and these results stored, the least-squares solution must be computed for each combination.

The problem of finding periodic waveforms in unevenly sampled data is ubiquitous in the field of astronomy, where much work has been done. It is easily seen that temporal frequencies in astronomical data can correspond to spatial toroidal mode numbers in tokamaks, and that unevenly sampled data in time is the analog of data from unevenly distributed Mirnov sensors in the toroidal coordinate. Since almost all astronomical data is unevenly sampled (due to weather conditions and the earth's rotation), considerable effort has gone into the problem of improving upon the limitations of the Lomb periodogram. For example, the CLEAN [7] and CLEANEST [8] algorithms attempt to

remove some of the artifacts arising from uneven sampling, to mention only two. In astronomy, the frequencies sought are obviously allowed to take on any value, which makes these methods not quite suitable for MHD analysis: periodic boundaries in toroids ensure that only modes with integer n can exist. (Again, n in toroidal space is the analog of frequency in a time series.)

Recently, a new method for fitting sinusoids to irregularly sampled data was proposed [9], which is implemented in the SparSpec computer code (freely available at: <http://www.ast.obs-mip.fr/Softwares>). The model used in SparSpec is linear in the frequency parameters: the data is modeled as a large number (possibly larger than the data size) of pure modes, discretized on a fixed, arbitrarily thin, grid. (For consistency with [9] we use the term ‘frequencies’ here, which applies to time-sampled data. For tokamaks and space-sampled data it corresponds to the spatial n -number.) Among the many representations fitting the data, we seek the one with the fewest non-zero amplitude, i.e. a sparse spectrum. The solution is computed as the minimizer of a penalized LS criterion:

$$J(x) = \frac{1}{2} \| \mathbf{y} - W\mathbf{x} \|^2 + \frac{\lambda}{\lambda_{Max}} \sum_{k=-K}^K |x_k|$$

with

$$\lambda_{max} = Max(W, g)$$

Here $\mathbf{y} = \{y_1, y_2, \dots, y_N\}^T$ is the vector of data taken at time t_n , W is a $N \times 2K+1$ matrix with elements $W_{n,k} = \exp(i2\pi t_n f_k)$, and $\mathbf{x} = \{x_{-K}, \dots, x_K\}^T$ is the vector of complex amplitudes associated with frequencies f_k , $k = -K \dots K$. The hyper-parameter λ is unknown and must be fixed to obtain a satisfactory sparse solution. It can be interpreted as the maximum peak amplitude allowed in the periodogram of the residual. This criterion is convex, with no local minima, but as it is not “strictly convex”, uniqueness of the global minimizer is not guaranteed. However, it is shown in [10] that the global minimizer is likely to be unique if it has less than $N/2$ non-zero components, where N is the data size. A computationally efficient and convergent optimization strategy has been proposed in [9], based on a Block Coordinate Descent algorithm. The minimization in SparSpec to detect frequencies and estimate the amplitude of the detected modes is performed on what is known as the l^1 -norm, which bypasses the requirement to test every possible combination of mode vectors as is the case with the l^0 -norm. Many theoretical works have been done to determine conditions of equivalence of both settings, one example is found in [11].

2. BENCHMARKING THE SPARSPEC METHOD FOR TOROIDAL MODE NUMBER ANALYSIS ON JET

Because SparSpec discretizes the allowable frequencies, it is ideally suited for toroidal mode number analysis, since only modes with integer wave number are sought, $f_k = k$, $k = -K \dots K$.

A batch processing code was developed for tokamak data in the following ways: first, the SparSpec code was adapted to take complex data as input. Then, because of the penalization term in $J(x)$, the

minimizing amplitudes are initially underestimated; the full version of SparSpec involves a re-estimation of the detected frequencies using barycentric arguments, which improves the frequency precision when the frequencies can be off the frequency grid. But in our case, we know that the frequencies are on the grid, so that instead a simple LS fitting routine was written to re-estimate amplitudes of the detected frequencies. The code was benchmarked with Monte Carlo simulations using artificial, noisy data. It was found to be very robust, and very fast (2 msec for one time point with 11 complex valued signals on a 2.2GHz processor).

On the JET experiment, there are eleven Mirnov coils at one common poloidal angle, unevenly spaced toroidally. The SparSpec method was applied to simulated data which mimicked data from JET, using identical sensor coordinates, with varying levels of noise. An example calculation is shown in Figure 1, where data was constructed from four random modes (random n , amplitudes, phases), and with 5% random Gaussian noise added to each sensor. The SparSpec frequency grid was restricted to $-40 < n < 40$. SparSpec correctly identifies the dominant four modes; the small amplitude solution is due to the added noise.

A systematic scan was then performed to benchmark the ability for SparSpec to resolve multiple modes in the Mirnov coil data. In the code, several parameters are set which facilitate better convergence and accuracy of the analysis, depending on the size of the input data array, the number of modes present in the data, the tolerance for precision, etc. The aim of the modeling was to find that set of parameters that would allow for an efficient and automated procedure for toroidal mode number separation. In particular, the results of SparSpec calculations are very sensitive to the hyper-parameter l . The size of the set frequency grid (range of n to consider) can also play a role in the accuracy of the calculations, and speed. Several levels of random noise were introduced to determine if and under what conditions SparSpec can be trusted. Some of the results of these simulations are shown in the following figures. In general, SparSpec produces very good results when the number of modes in the data is less than five, and when noise levels are reasonable (less than 10% of signal amplitudes). These results are consistent with the theoretical results which guarantee uniqueness of the criterion minimizer only if it has less than 5 non zero-components for $N=11$ data [10].

First, in order to qualitatively characterize the ability of SparSpec to determine toroidal mode amplitudes and phases, a set of artificial data was constructed which consisted of a ‘time’ series which included a superposition of 21 toroidal modes ($-10 < n < 10$), with varying amplitude and phases. Each mode has maximum amplitude at a unique time, in a Gaussian envelope. Each mode was designed to experience a full range of phases ($0-2\pi$ radians) within the time in which it had significant amplitude. Four different data sets were constructed, with different widths of Gaussian mode amplitudes, so that for different sets the amount of mode-overlap was varied. The more mode overlap, the greater the challenge to SparSpec, since it is expected to identify a larger number of simultaneous modes. The generated data contained no noise, i.e. the input to SparSpec represented ideal measurements of amplitude and phase at each sensor. One such data set is illustrated in Figure 2. SparSpec evaluated each set using six different values of the hyper-parameter, l . Other parameters

in SparSpec were held fixed, for example the frequency grid in which SparSpec searched was limited to $-30 < n < 30$.

The outcome of these calculations illustrates several trends as seen in Figure 3: when there is only one mode, nearly any λ value is adequate and SparSpec correctly identifies the amplitude and phase. (For real data with noise, the λ parameter should be set higher in order to preferentially suppress solutions containing multiple modes.) When there are several simultaneous modes, for λ values between 0.2 and 0.6, SparSpec correctly identifies the modes with the strongest amplitudes. This means that SparSpec is fairly robust, errors are expressed in the form of missing information about lower amplitude modes, and SparSpec does not indicate toroidal mode numbers which are not present in the input data. This trend however has limits, and with the addition of noise is only held true by higher values of the λ parameter. Fortunately, the general trend for higher λ 's is for SparSpec to ignore lower amplitude modes.

Next, in an attempt to quantify the accuracy of the SparSpec calculations, Monte Carlo type simulations were carried out, using the following scheme: randomly generated data sets with different mode numbers, phases, and relative amplitudes were input into SparSpec. Noise was included in the input data by generating Gaussian noise on each sensor. A noise figure of 10% represents the addition of a random number generated with a mean of 0, standard deviation 1, divided by 10, on each of the eleven sensors. In each case, the input mode amplitudes were normalized ($\sum |A_q| = 1$, $A_q =$ amplitude in q^{th} mode), and the error in the SparSpec output was evaluated by summing the difference between the input mode amplitudes and output amplitudes at all mode numbers, i.e.:

$$\sum_n |A_n^{\text{in}}| = 1 \quad , \quad \text{err} = \sum_{-n_{\text{max}}}^{n_{\text{max}}} |A_n^{\text{in}} - A_n^{\text{out}}|$$

If $\text{err} \geq 0.5$, the calculation was considered to be 100% wrong. This is a very conservative way of estimating errors because an error for one mode number can throw the entire result into the 100% error bin, even though there may be several modes which SparSpec has identified correctly. Monte Carlo type simulations then produced results which were histogrammed as shown in Figure 4. Evident in the figure is the fact that SparSpec either correctly identifies all the modes and their amplitudes and phases, with little error, or completely misses the mark. This can be understood by recognizing that there are several solutions (with vastly different n 's and amplitudes) which come close to reproducing the input data.

1000 calculations were performed for 10 different noise levels, 4 different n -number ranges, and 6 different input data types (from having only one n present to finally six distinct modes). The result of one subset of the calculations is shown in Figure 5. The full set of results is shown in a set of bar charts in Figure 6. The general conclusions are that SparSpec can handle up to 5 simultaneous modes when the noise level is effectively 0. In the presence of sensor noise, SparSpec calculations are mostly correct when there are four or less modes present in the data even when the mode spectrum contains $n \leq 40$; a greater number of modes in the output should probably not be trusted.

3. RESOLVING STABLE ALFVÉN EIGENMODES ON JET

One area in which the detailed mode number identification of MHD fluctuations is desired is known as MHD spectroscopy [12]. The term refers to a broad topic in which fluctuations are used to deduce information about bulk plasma parameters, for example some properties of the q-profile are revealed with the observation of reversed-shear Alfvén eigenmodes. The TAE antenna project on JET [13,14,15] is an example of active MHD spectroscopy, where small magnetic perturbations are actively produced by external antennas, and the plasma response yields information about toroidal (and other classes) of Alfvén eigenmodes (AE's). The motivation is that multiple AE's with several toroidal mode numbers are known to be excitable by supra-thermal ion populations, which in some circumstances can lead to rapid loss of fast particle confinement [16,17]. This would pose problems for a burning plasma scenario, and therefore measuring the damping rates of AE's in the absence of fast particle drive and in a variety of plasma conditions will aid in understanding some underlying physics relevant to burning fusion plasmas.

The TAE antennas on JET consist of an array of small coils which can excite medium and high-n Alfvén Eigenmodes, depending on the polarity of the individual antennas (one amplifier is the common source). Because of the small spatial extent of the antenna arrays (see Figure 7), the magnetic perturbations to the plasma surface necessarily are composed of a broad spectrum of toroidal mode numbers (Figure 7, right). Data from Mirnov coils are obtained via synchronous detection hardware, i.e. a very sharp bandpass filter (± 100 Hz) produces the in-phase and quadrature signal components only at the antenna frequency, and these signals are then used to facilitate real time resonance detection and tracking [8]. The damping rate of the detected resonant mode is determined post-shot by evaluating the poles and residues in the transfer function between Mirnov signals and antenna currents [13].

On JET, for unstable modes driven by fast ions, multiple AE's with medium toroidal mode numbers ($3 < n < 12$) typically oscillate with nearly the same frequency of a few $100 \times$ kHz, with the observed frequencies in the lab frame separated by a small doppler shift due to plasma rotation (since the mode rotates with the plasma fluid, $\Delta f = \Delta n \times \Omega$), typically by a few kHz. This is enough to determine toroidal mode numbers separately at each frequency using standard techniques. But for the case of stable, externally excited AE's, any modes near resonance with the driving frequency will be excited (at that same frequency).

In the presence of only one dominant resonant mode, n-number identification is straight forwardly accomplished with straight-line phase fitting. The resonances of other, less dominant (more stable or more core-localized) modes with different n-numbers will be missed, however. In addition, when the phase-fit is very bad or jumps from one n to another with incremental changes in frequency, it is a strong indication that there are several modes being detected simultaneously (see Figure 8). This latter case can completely prevent n-number identification by traditional methods such as straight line phase-fitting.

Using SparSpec, individual MHD modes can be resolved and the damping rates determined for

each mode separately. Only then can the damping rate for individual modes be calculated accurately, without being obscured by other modes with similar resonant frequencies but different damping rates. An example is shown in Figure 9 for JET Pulse No: 69586, in which three toroidal AE's with mode numbers $n = -1, 0, 2$ exist simultaneously near $t = 32$ sec.

When a very small time interval is analyzed, the changes in amplitude and phase of an individual mode as a function of incremental changes in antenna frequency can be used to calculate the damping rate, γ , of the mode in that time interval [13]. One such calculation is shown in Figure 10, for $t \approx 31.8$ sec. When plotting the in-phase and quadrature (real and imaginary) components in the complex plane, a circle results. It is interesting to note that the resonant frequencies of the three AE's differ slightly from each other, based on the fact that for each mode the peak amplitude occurs at slightly different times. The damping rates of the three modes in this case are nearly identical ($\gamma/\omega \approx 2\%$). Such information would not be possible without applying the SparSpec method to the Mirnov data first.

4. FURTHER CONSIDERATIONS

While perhaps obvious, nevertheless important to note is that in the presence of significant variation across sensors in terms of frequency dependent complex gain (amplitude and phase), the SparSpec method no longer produces correct toroidal mode numbers. Such differences may be the result of conducting structures nearby individual probes, subject to different eddy current patterns, or due to differences in probe construction or electrical transmission line characteristics. Thus, for accurate toroidal mode number reconstruction the transfer function of each individual probe must be known, and the data calibrated, at least relatively. Of course, this is also the case for any other mode number identification method. For the magnetic probes on JET, uncertainties in the relative calibration of Mirnov coils at high frequencies lead to systematic errors in the analysis, so for example pure low- n modes will appear to be accompanied by a small amplitude high- n mode (e.g. $n = 29$) at high frequencies. To thoroughly discuss these errors is beyond the scope of this paper; suffice it to say that such errors are small for JET data below 300kHz.

Another topic which is of some importance in evaluating the abilities of SparSpec deals with the spacing and positioning of individual Mirnov coils, as well as the number of coils available for use. Of course the probe positions on JET are fixed, but such an investigation might be worthwhile in view of the (not yet completed) design of the magnetic probe diagnostics for ITER. Again it is well beyond the scope of this paper to investigate these topics in any systematic way, because optimized sampling strategy is a topic of some depth, the reader is referred to [3] for a detailed treatment.

For illustrative purposes, an example of the effect of sensor positioning will be described. In the modeling of artificial data, it was observed that SparSpec produces very small artifacts near $n = +/- 10$ and $+/- 20$, i.e. the output contains small peaks at various mode numbers when the input data contains modes $n = 9, 10, 11$. These false peaks, while negligibly small, seem to be result from the toroidal arrangement of the sensors. They can be understood by considering that for regularly spaced coils, the spectral window is a Dirichlet kernel of period N , where N is the number of coils.

In the irregular sampling case (such as at JET), the spectral window also can have secondary lobes, due to a hidden regularity in the sampling: 8 of the 11 sensors in use on JET actually form part of an array of 10 equally spaced Mirnov coils. Using simulated data, when the sensor spacing is optimized according to results by Madore and Freedman (Table 1 in [18]), SparSpec output calculations do not exhibit any errors of the kind described. A more noticeable difference in performance emerges when processing data which contains some amount of noise and is discernable in Figure 11. This figure depicts SparSpec output data in the same fashion as Figure 3 in section 2. Two scenarios were run: one in which the sensor geometry is JET like (a), and one in which the spacing of eleven sensors was “optimized” (b). The JET geometry result has a few more errors, particularly concerns the phases (c). The optimized geometry also allows slightly better resolution into lower amplitudes, as seen by studying the figures closely.

CONCLUSION

A new method for identifying toroidal mode numbers in Mirnov data from toroidal plasmas has been benchmarked. Embodied in the SparSpec code, and originally developed for analysis of unevenly time-sampled astronomical data, this new method fits signals which are unevenly sampled in the toroidal coordinate to a sum of an arbitrarily large number of toroidal modes with integer mode numbers. By assigning a larger penalty to solutions that invoke larger numbers of modes, SparSpec determines the best fit with the sparsest spectrum. The method has proven to be extremely robust, and is especially useful for resolving the amplitudes and phases of multiple Alfvén eigenmodes which are ringing with the same or nearly the same frequency. The method also is superior in determining n-numbers when there is only one dominant mode present, as compared with traditional straight line phase-fitting techniques, because both amplitude and phase information is considered, and thus discrimination against noise is improved.

The great efficiency with which SparSpec detects multiple modes in large datasets suggests that it may be used in real-time applications such as Resistive Wall Mode (RWM) or tearing mode control, among others. We plan to use SparSpec in feedback calculations to target specific n-numbered modes during active Alfvén spectroscopy, using a subset of 8 Mirnov coils, and with the goal of loop rates ≤ 1 msec.

Examples involving stable Alfvén eigenmodes in JET, excited by an array of external antennas, were used to illustrate the efficacy of the method. Additional general considerations regarding optimized spatial sampling strategies were also briefly addressed.

Acknowledgement:

This work is partially supported by US DOE Grant DEFG02-99ER54563.

REFERENCES:

- 1]. J.S. Kim et al., Plasma Phys. Control. Fusion **41** (1999) 1399

- [2]. P. Zanca et al., Phys. Plasmas **8** (2001) 516
- [3]. F. Marvasti, “Nonuniform Sampling: Theory and Practice” (2001) Springer
- [4]. N.R. Lomb, Astrophysics and Space Science **39** (1976) 447
- [5]. S. Zegenhagen, A. Werner et al., Plasma Phys. Control. Fusion **48** (2006) 1333
- [6]. M. Hole, L. Appel, Plasma Phys. Control. Fusion **49** (2007) 1971
- [7]. D. Roberts, J. Lehar and J. Dreher, The Astronomical Journal, **93** (1987)
- [8]. G. Foster, Astronomical J. **109** (1995) 1889
- [9]. S. Bourguignon, H. Carfantan, T. B^hm, Astronomy and Astrophysics **462** (2007) 379
- [10]. S. Bourguignon, H. Carfantan, J. Idier, IEEE Selected Topics in Sig. Proc. **1** (2007) 4.
- [11]. D. Donoho, J. Communications on Pure & Applied Math. **59** (2006) 797
- [12]. A. Fasoli et al., Plasma Phys. Control. Fusion **44** (2002) B159
- [13]. A. Fasoli et al., Phys. Rev. Lett. **75**, (1995) 645
- [14]. A. Fasoli et al., Phys. Plasmas **7** (2000) 1816
- [15]. D. Testa et al., 23rd Symposium on Fusion Technology, Venice (Italy), September 2004
- [16]. K. Wong, Phys. Rev. Letters **14** (1991) 1874
- [17]. W. Heidbrink et al., Plasma Phys. Control. Fusion **45** (2003) 983
- [18]. B.F. Madore and W.L. Freedman, The Astrophysical Journal **630** (2005) 1054

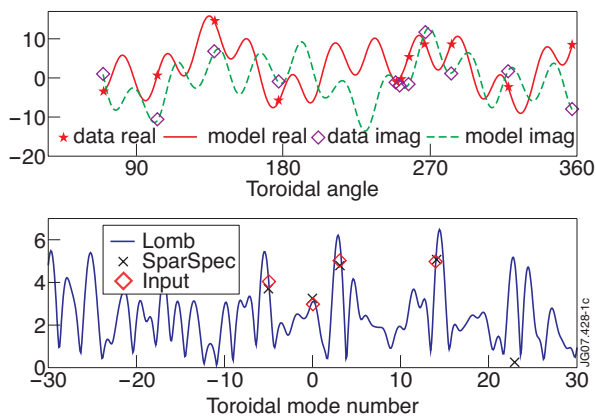


Figure 1: SparSpec calculation using simulated data: top: data (points) and model fit (lines). Bottom: input mode amplitudes versus estimation from SparSpec, along with Lomb periodogram.

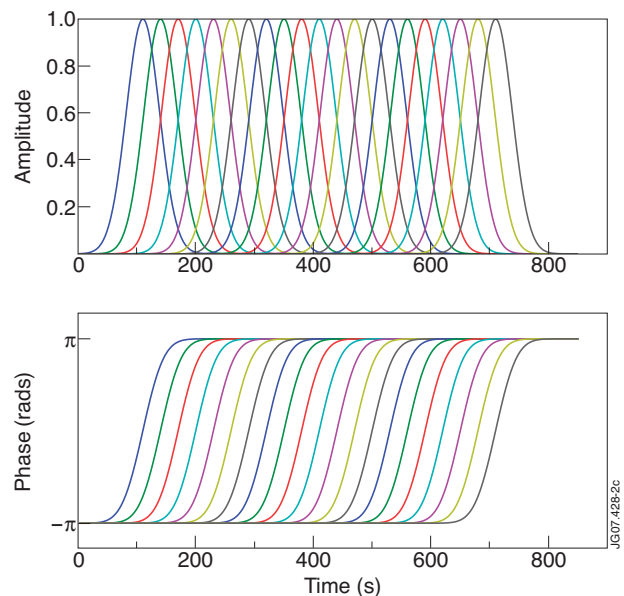


Figure 2: Amplitude and phase of input data for simulated time series. Different colors correspond to different n -numbers, consecutively increasing starting with $n = -10$. The data shown here feeds into SparSpec an average of six modes to identify at any given time, for width $\sigma = 30 = \text{number of time points between half width / half maximum}$. Other data sets used had less mode overlap.

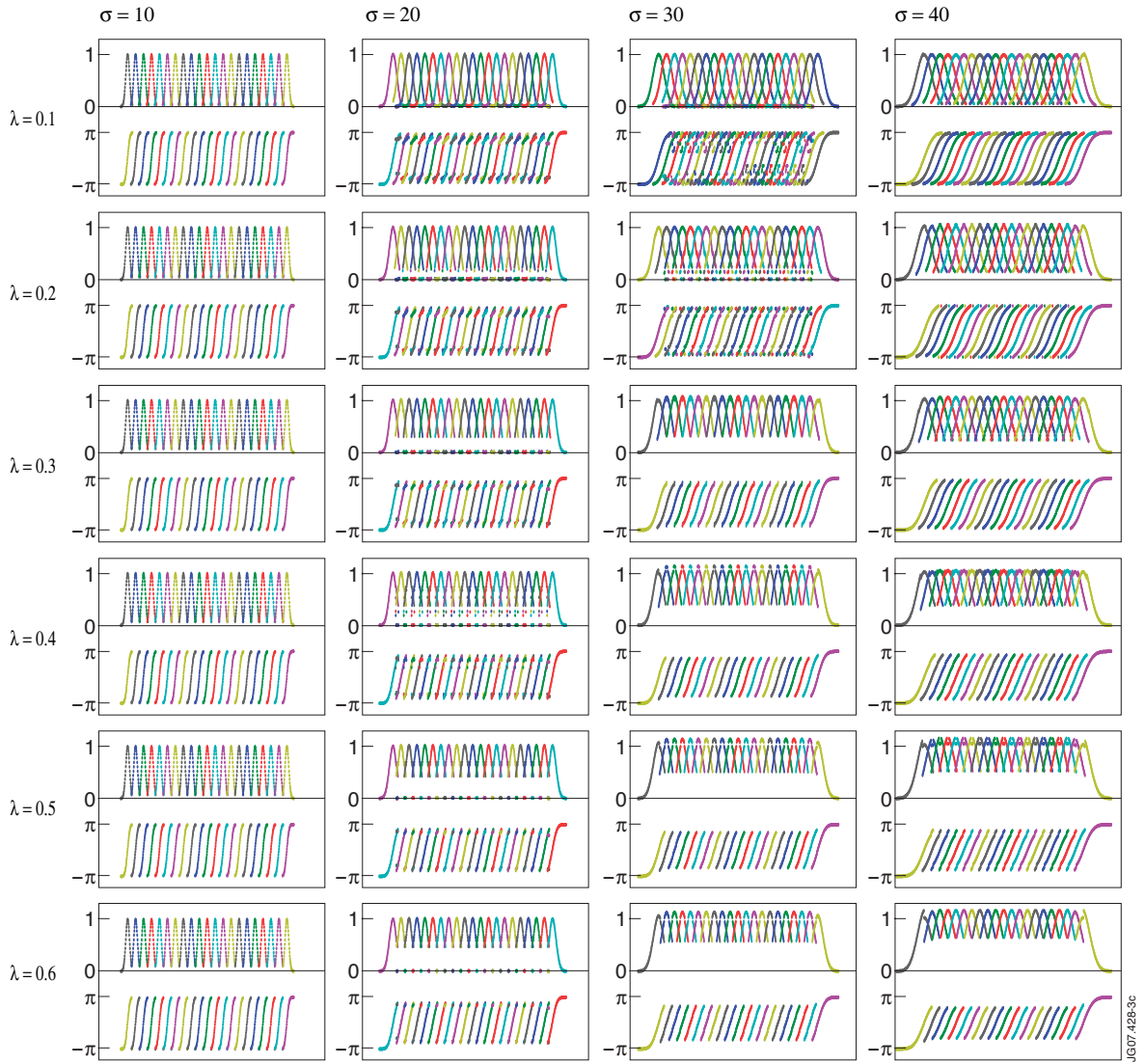


Figure 3: SparSpec estimations for noiseless input data, $-10 < n < 10$, for a range of l parameter, and four levels of “difficulty”. Good performance is characterized by good reproduction of Figure 2 in each plot.

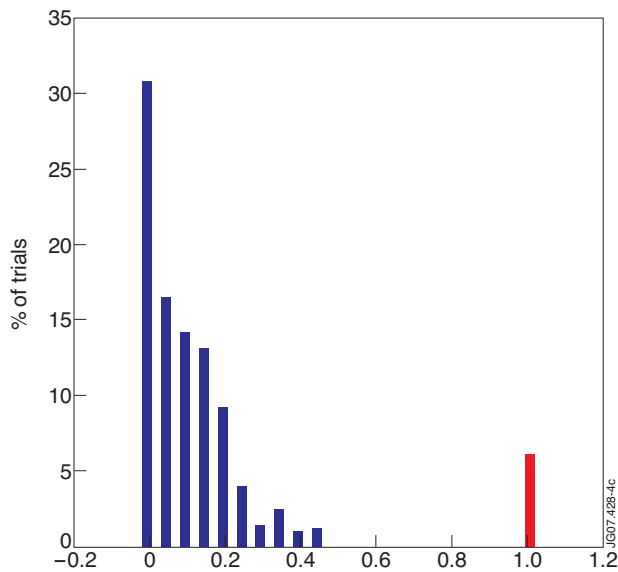


Figure 4: Result of 1000 simulations with 3 modes included in input, comprised of random n 's ($-40 < n < 40$), amplitudes, and phases, with 5% noise, fixed $\lambda=0.5$. Errors greater than 0.5 are binned into “1”, represented by red bar.

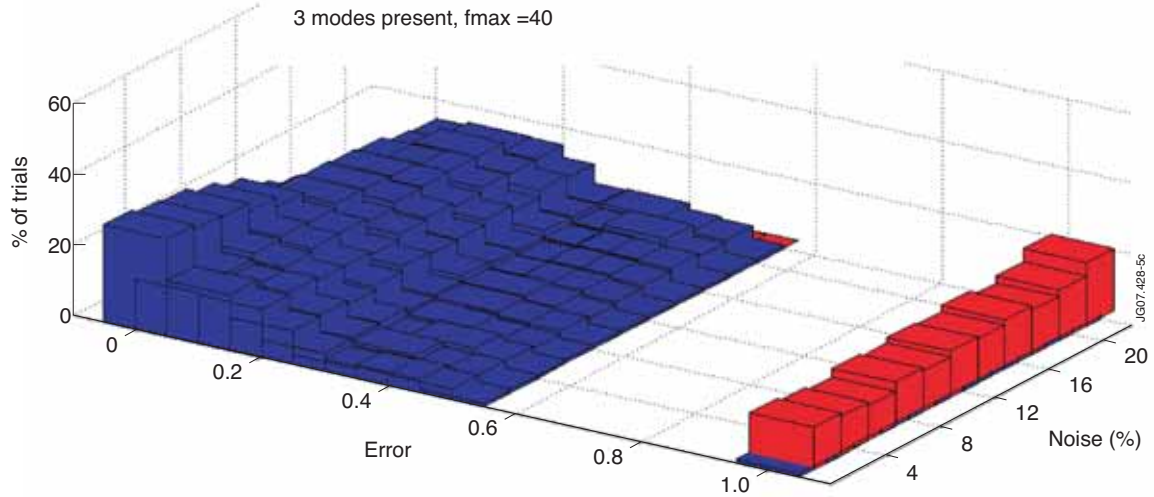


Figure 5: Error statistics for 2 random modes, $-40 < n < 40$, versus noise level, fixed $\lambda/\lambda_{max} = 0.5$. SparSpec correctly separates modes 94% of the time, even if there is 20% noise present in the data.

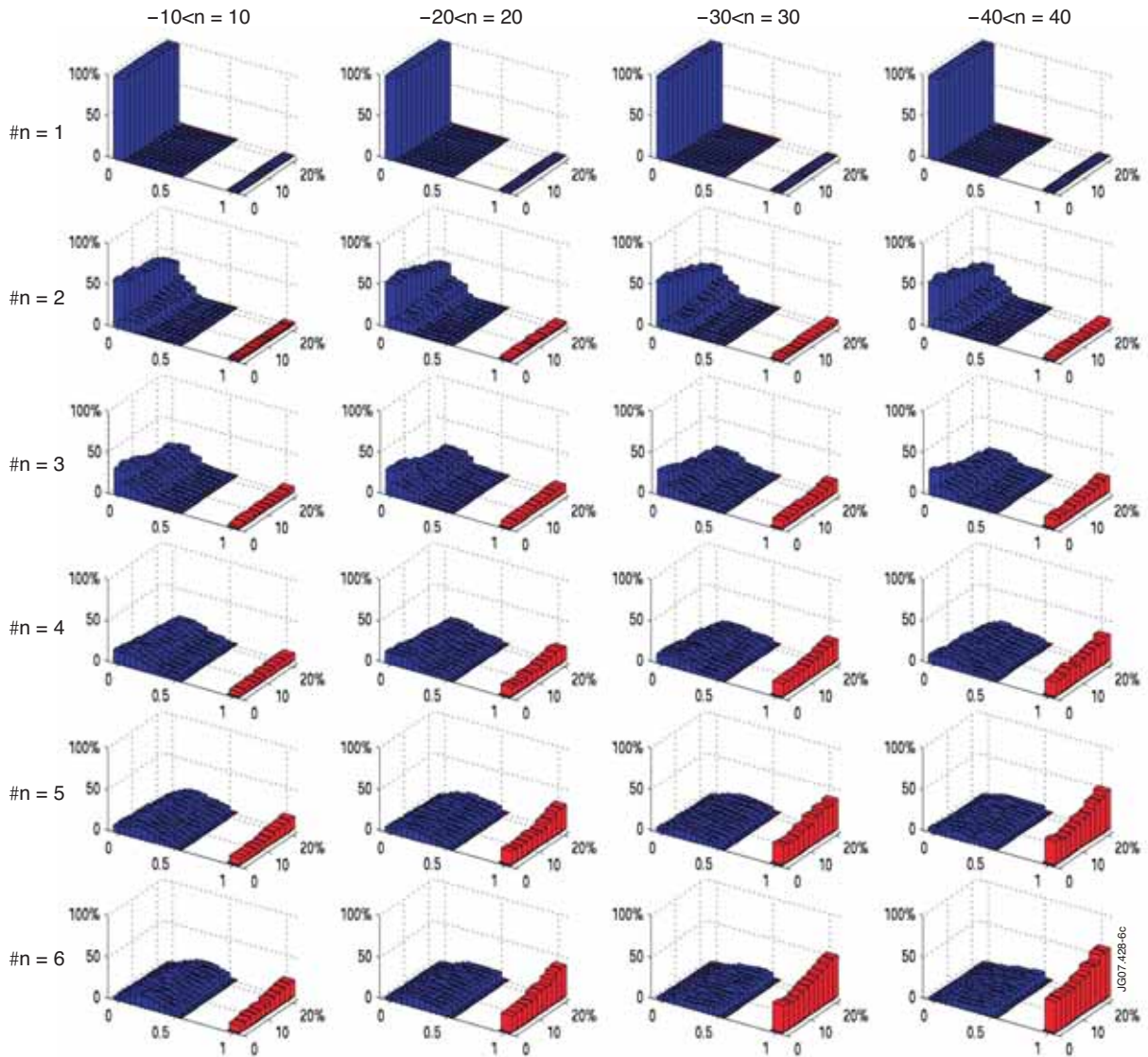


Figure 6: Error results for many noise levels, numbers of modes contained in the data, and maximum mode number included in the data sets ($= \max n$ sought), fixed $\lambda/\lambda_{max} = 0.5$.

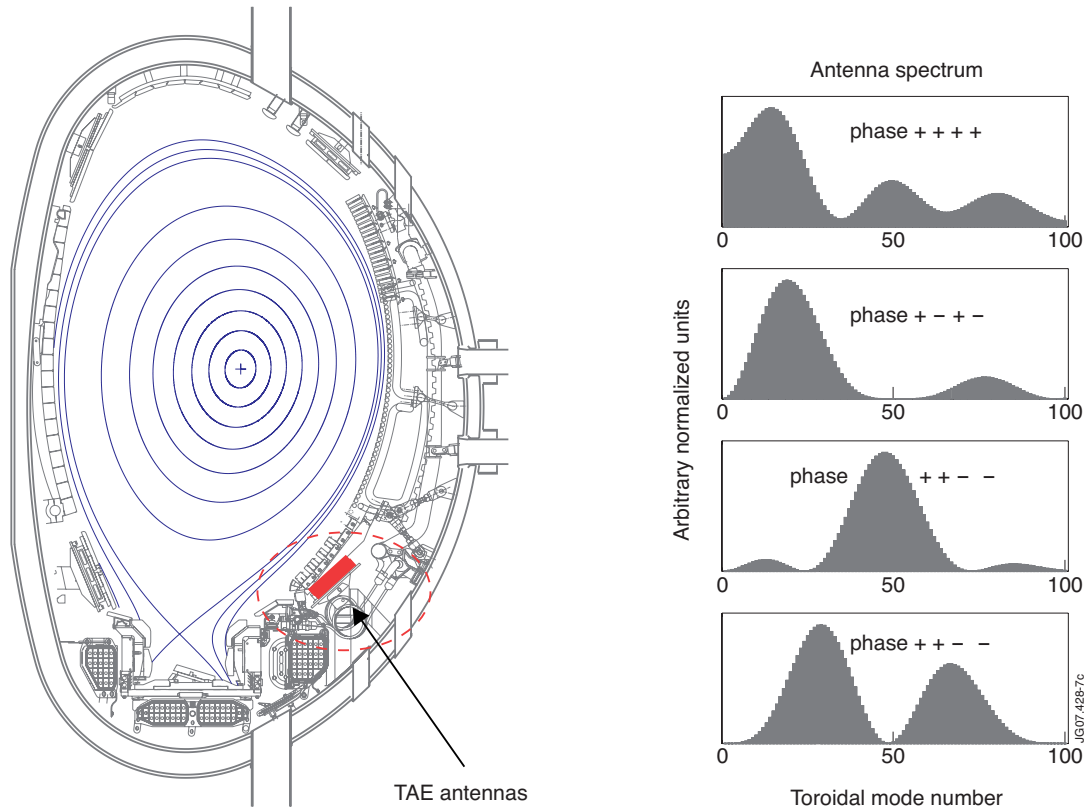


Figure 7: Left: active MHD antenna location in the JET tokamak. Right: calculation of approximate toroidal mode spectra (only positive n shown) being driven in vacuum with four different antenna phase configuration.

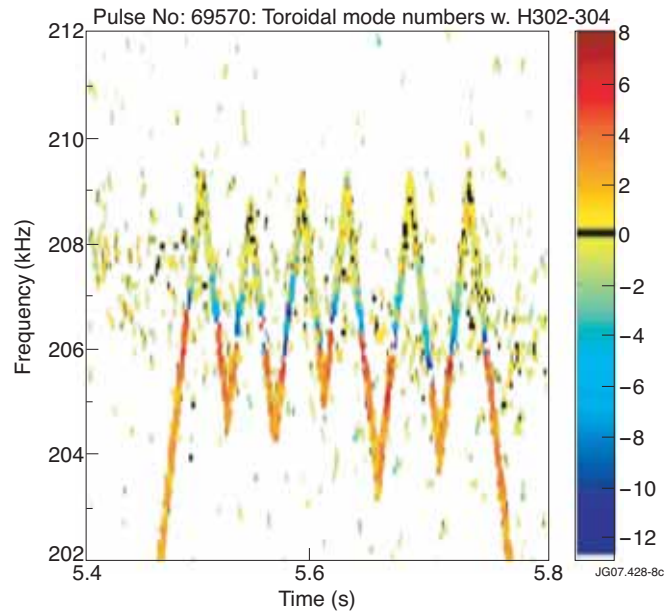


Figure 8: Stable TAE's excited by external antennas in JET Pulse No: 69570. Active antennas sweep in frequency to repeatedly scan over a detected resonance. Determination of n -number using simple straight line phase-fitting of three closely spaced Mirnov coils shows drastic jumps in n -number for incremental frequency changes and indicates the presence of multiple modes.

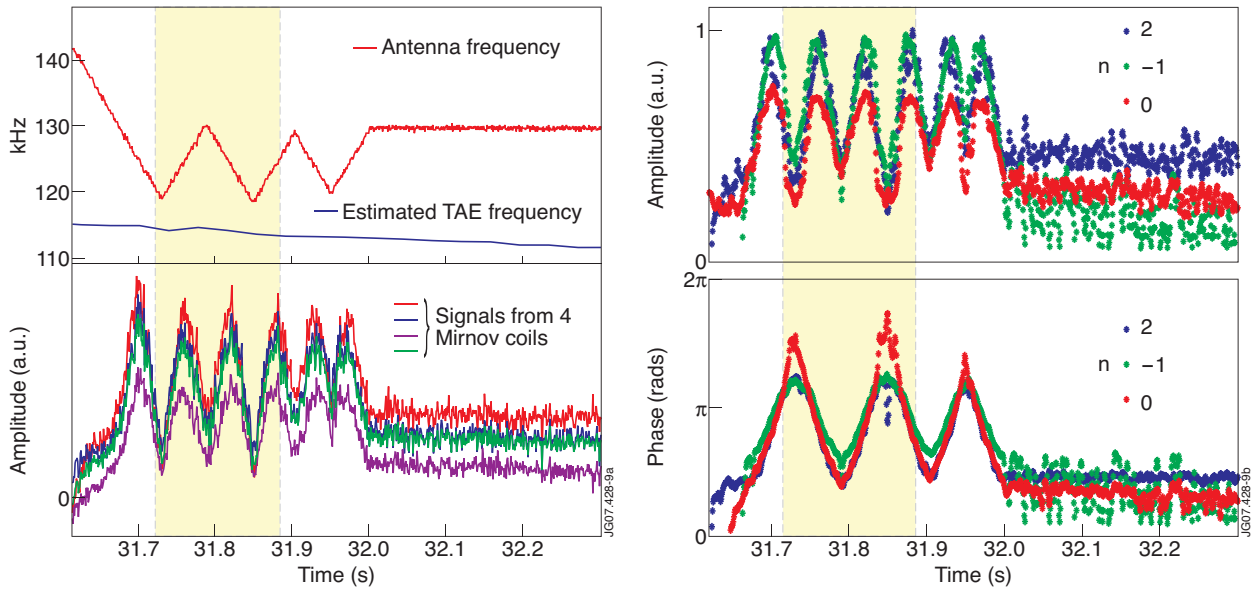


Figure 9: Left: detail of JET Pulse No: 69586 from $31.6 < t < 32.3$. Three modes with $n = -1, 0, 2$ compete with nearly equal amplitudes. Right: SparSpec resolves amplitude and phase of each mode.

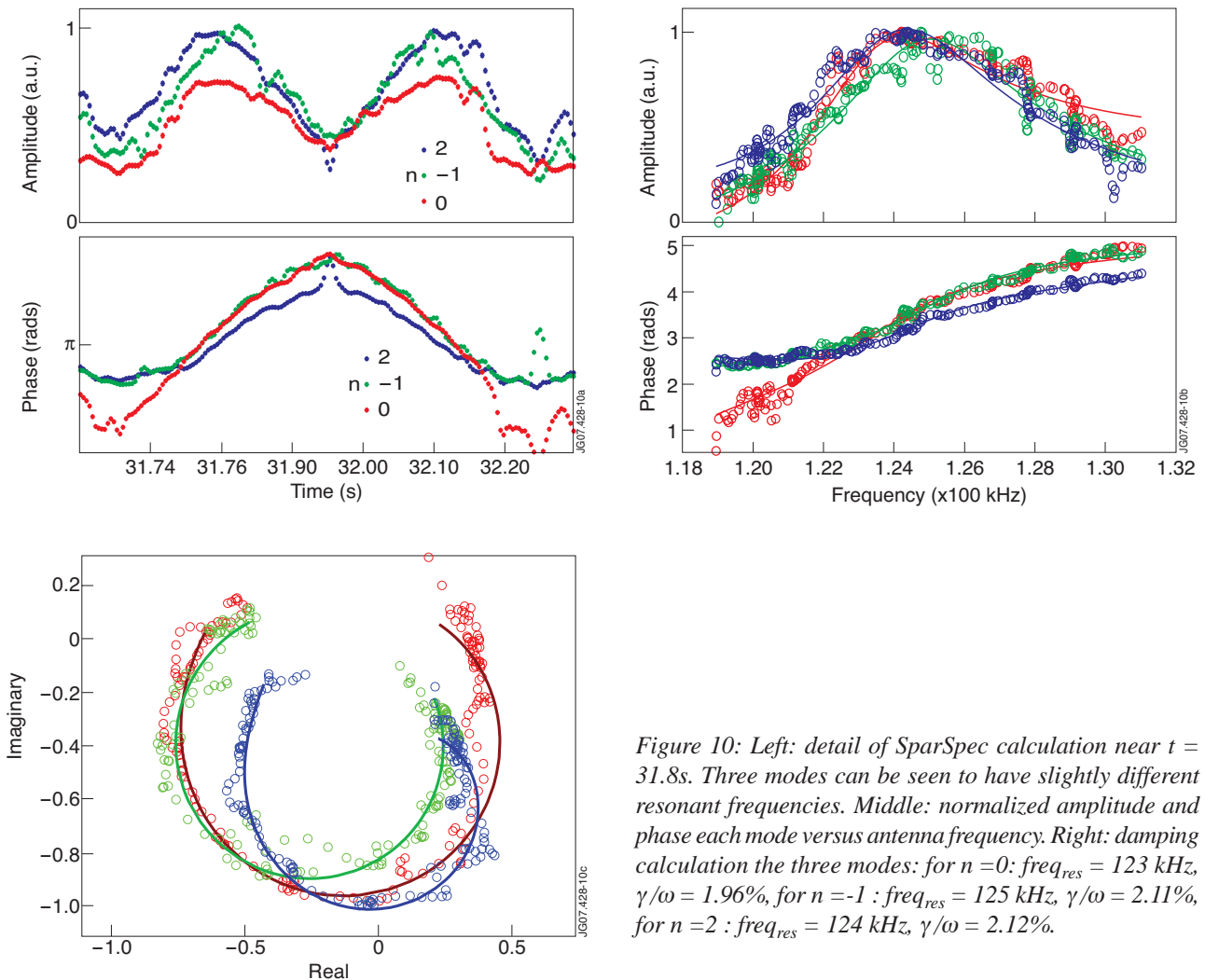


Figure 10: Left: detail of SparSpec calculation near $t = 31.8s$. Three modes can be seen to have slightly different resonant frequencies. Middle: normalized amplitude and phase each mode versus antenna frequency. Right: damping calculation the three modes: for $n=0$: $freq_{res} = 123 \text{ kHz}$, $\gamma/\omega = 1.96\%$, for $n=-1$: $freq_{res} = 125 \text{ kHz}$, $\gamma/\omega = 2.11\%$, for $n=2$: $freq_{res} = 124 \text{ kHz}$, $\gamma/\omega = 2.12\%$.

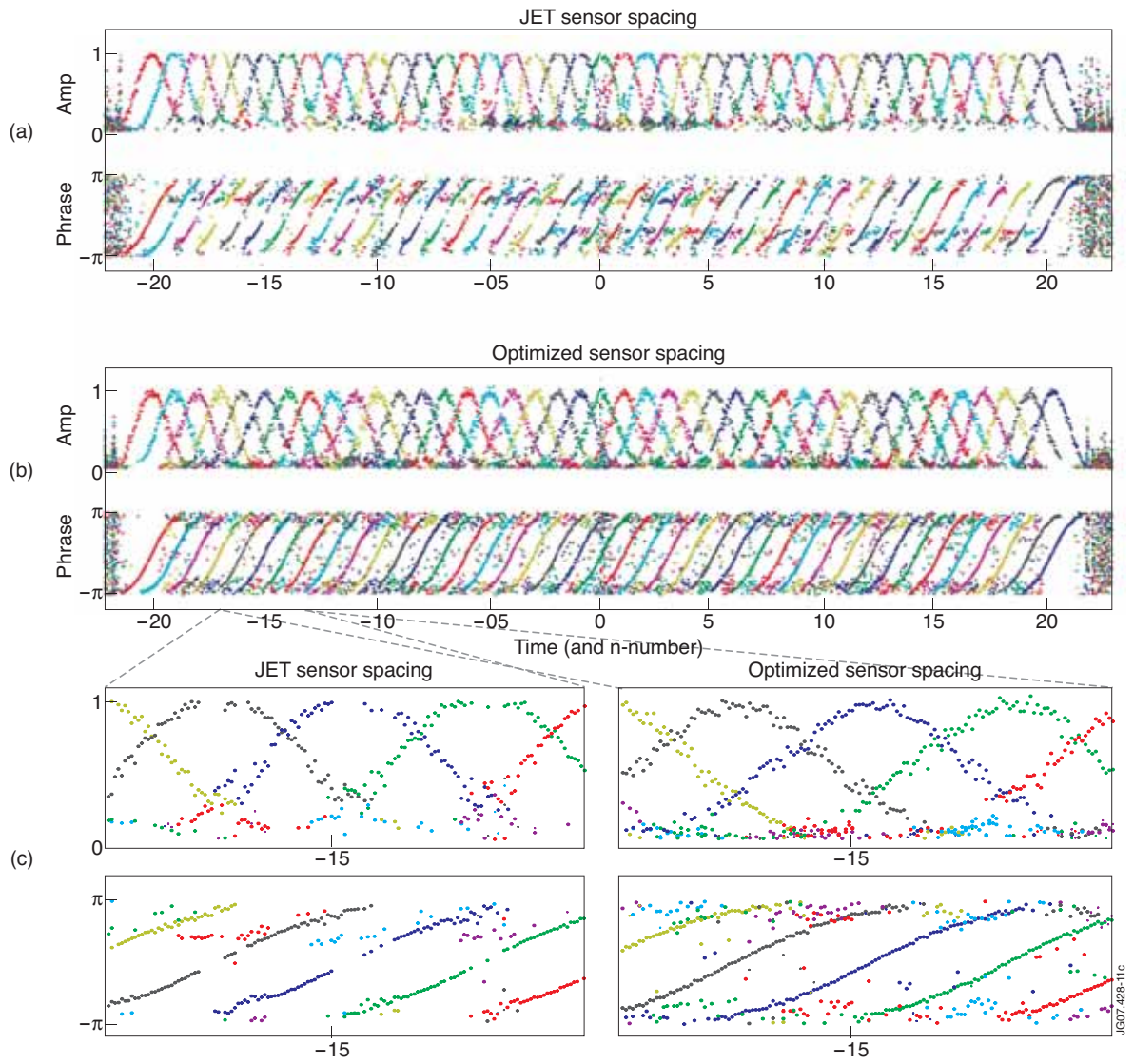


Figure 11: SparSpec calculations estimations for input data with 5% noise, $-20 < n < 20$, l is fixed at 0.4. Interpretation as in Figure 3. (a) output using JET sensor geometry, (b) output using suggested sensor spacing from [18]. (c) Zoom detail of amplitudes (left) and phases (right) showing minor benefits of optimum spacing.